

Field induced spin exciton doublet splitting in $d_{x^2-y^2}$ -wave 115-heavy electron superconductors

Alireza Akbari* and Peter Thalmeier

Max Planck Institute for the Chemical Physics of Solids, D-01187 Dresden, Germany

(Dated: May 24, 2021)

We investigate the spin-exciton modes in the superconducting $d_{x^2-y^2}$ state of CeMIn₅ heavy fermion compounds found at the antiferromagnetic wave vector by inelastic neutron scattering. We present a theoretical model that explains the field dependence for both field directions. We show that the recently observed splitting of the spin exciton doublet in CeCoIn₅ into two non-degenerate modes for in-plane field appears naturally in this model. This is due to the spin anisotropy of g-factors and quasiparticle interactions which lead to different resonant conditions for the dynamic susceptibility components. We predict that the splitting of the spin resonance doublet becomes strongly nonlinear for larger fields when the energy of both split components decreases. For field along the tetragonal axis no splitting but only a broadening of the resonance is found in agreement with experiment.

PACS numbers: 74.25.Jb, 71.27.+a, 72.15.Qm

I. INTRODUCTION

In unconventional superconductors quasiparticle excitations that determine low temperature thermodynamics and response exhibit a generally anisotropic gap $\Delta(\mathbf{k})$ with possible node lines on the Fermi surface (FS). In addition to these single particle excitations collective excitations may appear. The collective oscillation of the superfluid density or 'Higgs mode' that belongs to the singlet spin sector is difficult to observe. In addition collective spin triplet excitations may be present below the gap edge that are formed as bound states due to quasiparticle interactions. They are accessible directly by inelastic neutron scattering (INS) and have been found in a considerable number in unconventional superconductors. In heavy fermion compounds their typical energy is in the range of just one meV. The most clearcut example belongs to the class of 115 superconductors, CeMIn₅ (M= Rh, Ir and Co). They have attracted great interest because of coexisting and competing antiferromagnetic (AF) and superconducting (SC) states¹⁻⁴, and in particular due to the possible existence of a Fulde-Ferrell-Larkin-Ovchinnikov (FFLO) phase in CeCoIn₅⁵.

The highest superconducting critical temperature of this family appears in CeCoIn₅ with $T_c = 2.3\text{K}$, and the question of the gap symmetry in these compounds has been intensely discussed⁶⁻⁸. A powerful indirect method to study the unconventional gap symmetry is provided by the spin resonance peak which may appear in inelastic neutron scattering (INS). Such a pronounced spin resonance has been observed in CeCoIn₅ and La substituted crystals at $\omega_r/2\Delta_1 = 0.65$ in the superconducting state by INS where $2\Delta_1$ is the main quasiparticle gap obtained from tunneling experiments⁹. It is confined to a narrow region around the AF wave vector $\mathbf{Q} = (\frac{1}{2}, \frac{1}{2}, \frac{1}{2})^{10}$. A theoretical calculation of the dynamical spin response using realistic Fermi surface¹¹

shows that the resonance can appear only for the $d_{x^2-y^2}$ -wave gap symmetry but not for d_{xy} -type gap because the precondition $\Delta(\mathbf{k} + \mathbf{Q}) = -\Delta(\mathbf{k})$ for a spin resonance¹² is only fulfilled in the former case. Indeed the $d_{x^2-y^2}$ gap symmetry has also been found by thermal conductivity⁷ and specific heat measurements⁸ in rotating magnetic fields.

The existence of a spin exciton resonance in the SC phase is a well established many-body effect which has also been observed in other unconventional superconductors like high-Tc cuprates¹³, heavy fermion metals UPd₂Al₃¹⁴⁻¹⁶ and CeCu₂Si₂^{17,18}, and in particular in many Fe-pnictide compounds¹⁹. The appearance of the resonance depends sensitively on the type of unconventional Cooper-pairing and provides a powerful criterion to eliminate certain forms of pairing when a resonance is observed. These interpretations, however, all depend considerably on theoretical phenomenological model features like FS nesting properties, nodal positions and momentum dependence of the gap as well as the size and anisotropy of quasiparticle interactions.

The spin exciton is a triplet excitation in the isotropic case since it should appear as a pole or resonance in all three components of the susceptibility tensor. In principle, in presence of the magnetic field it should split into three modes with different polarization (left and right handed as well as longitudinal). The field-induced splitting of spin excitons has been predicted for the cuprates²⁰ but was so far never identified experimentally in any unconventional superconductor.

Recently an apparent field induced spin-exciton splitting has been found for the first time in CeCoIn₅ by INS and has given rise to an interesting debate. In Ref. 21 a splitting into two (rather than the expected three) modes was found for field in the tetragonal plane and no splitting for perpendicular field. On the other hand no splitting was reported in Refs. (22 and 23) for both field directions and only an increased broadening of the peak is observed²². Furthermore it has been pro-

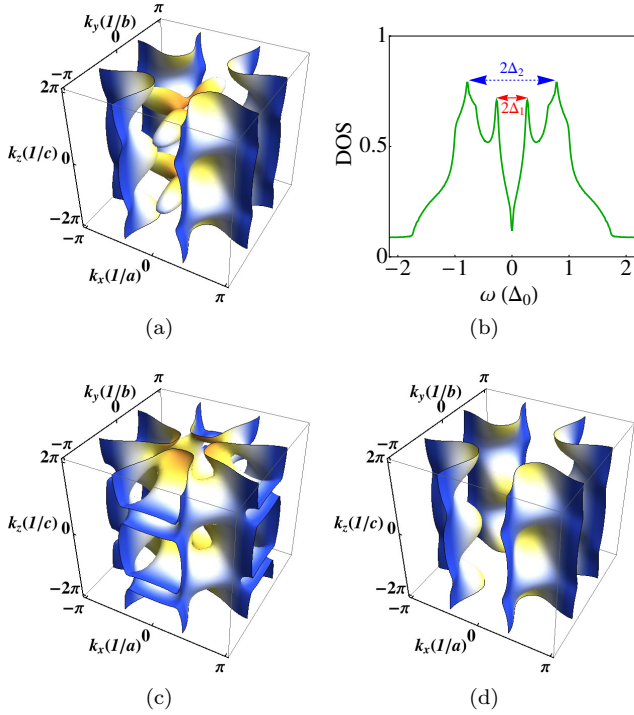


FIG. 1. (Color online) Fermi Surface (a) and quasiparticle density of states (b) for zero magnetic field, here $2\Delta_1 = 0.56\Delta_0$ and $2\Delta_2 = 1.5\Delta_0$. (c) and (d) show Fermi surfaces for spin up and spin down, respectively, in presence of the magnetic field $B_0\hat{z}$, corresponding to Zeeman energy splitting $h_{B_0}^f = g_{\parallel}^f \tilde{\chi} \mu_B B_0 = 0.3\Delta_0$ which is also used in subsequent figures.

posed that the FFLO-type inhomogeneous superconducting ‘ \mathbf{Q} -phase’^{24–27} is due to the condensation of the lower split-off branch of spin excitons close to the upper critical field^{21,28}.

In this paper we present a theoretical analysis to address the field splitting of the spin resonance which have been observed recently in INS experiments²¹ for the first time in an unconventional superconductor. We investigate whether the conventional picture of this mode as a triplet bound state of quasiparticles can explain these observations. We clarify the appropriate conditions for the splitting to occur for the different field directions as well as the number and field dependence of the split spin exciton modes.

II. THEORETICAL MODEL

The Anderson lattice model provides a convenient frame to model the heavy quasiparticle bands in CeMIn_5 realistically²⁹. The electronic structure of CeMIn_5 has been investigated by using tight binding models with effective hybridisation for f-electrons and c-(conduction) electrons^{29,30}. The crystalline electric field (CEF)-splitting is approximately three times larger than the

quasiparticle band width ($W \approx 4$ meV), then one may restrict the model to consider the lowest $\Gamma_7^{(1)}$ Kramers doublet of 4f states³¹. This can be described by a pseudo-spin $\sigma = \uparrow\downarrow$ degree of freedom. Choosing its quantization axis along the \hat{z} direction which is defined by the magnetic field, the Anderson lattice model Hamiltonian for the two hybridized conduction and localized orbitals (c,f) which are doubly Kramers degenerate is given by

$$\mathcal{H} = \sum_{\mathbf{k}\sigma} \varepsilon_{\mathbf{k}\sigma}^c c_{\mathbf{k}\sigma}^\dagger c_{\mathbf{k}\sigma} + \varepsilon_{\mathbf{k}\sigma}^f f_{\mathbf{k}\sigma}^\dagger f_{\mathbf{k}\sigma} + V_{\mathbf{k}} \left(c_{\mathbf{k}\sigma}^\dagger f_{\mathbf{k}\sigma} + h.c. \right) + \sum_{\mathbf{k}\mathbf{k}'} U_{ff} f_{\mathbf{k}\uparrow}^\dagger f_{\mathbf{k}'\downarrow}^\dagger f_{\mathbf{k}'\downarrow} f_{\mathbf{k}\uparrow}. \quad (1)$$

Where $c_{\mathbf{k}\sigma}^\dagger$ creates an electron with spin σ in the conduction orbital with wave vector $\mathbf{k} = (k_x, k_y, k_z)$. Furthermore, $\varepsilon_{\mathbf{k}\sigma}^c = \epsilon_{\mathbf{k}}^c - \mathcal{H}_B^c$ and $\varepsilon_{\mathbf{k}\sigma}^f = \epsilon_{\mathbf{k}}^f - \mathcal{H}_B^f$, where $\epsilon_{\mathbf{k}}^c$ and $\epsilon_{\mathbf{k}}^f$ are effective tight binding dispersions of the conduction band and the renormalized dispersion for the f band, respectively. The Zeeman splittings of bands due to the effective molecular fields are given by $\mathcal{H}_B^c = h_B^c \sigma_z$ with $h_B^c = \frac{1}{2} g^c \tilde{\chi} \mu_B B$ and $\mathcal{H}_B^f = h_B^f \sigma_z$ with $h_B^f = \frac{1}{2} g_{\alpha}^f \tilde{\chi} \mu_B B$. Here σ_z is the Pauli matrix, B is the magnetic field, g^c is the g-factor for c-electrons, g_{α}^f the g-factor for f-electrons in direction $\alpha = \parallel, \perp$ with respect to the tetragonal plane, $\tilde{\chi}$ the Stoner enhancement factor of the homogeneous susceptibility due to quasiparticle interactions and μ_B is the Bohr magneton. The anisotropy of the g-factors is obtained from that of magnetization or spin susceptibility³² as $g_{\perp}^f/g_{\parallel}^f = 2.3$ assuming that the f-electron contribution in the magnetization dominates. For that reason we chose a small $g^c/g_{\parallel}^f = 0.2$. Furthermore $f_{\mathbf{k}\sigma}^\dagger$ creates the f-electron with momentum \mathbf{k} and pseudo spin σ , and U_{ff} is its on-site Coulomb repulsion. Finally $V_{\mathbf{k}}$ is the hybridization energy between the lowest 4f doublet and conduction bands which contains implicitly the effect of spin orbit and the CEF term and is taken as momentum independent.

It is known²⁹ that in the limit of $U_{ff} \rightarrow \infty$ where double occupation of the f-states are excluded, an auxiliary boson defines the mean field (MF) Hamiltonian as^{33,34}

$$\mathcal{H} = \sum_{\mathbf{k}\sigma} \varepsilon_{\mathbf{k}\sigma}^c c_{\mathbf{k}\sigma}^\dagger c_{\mathbf{k}\sigma} + \tilde{\varepsilon}_{\mathbf{k}\sigma}^f f_{\mathbf{k}\sigma}^\dagger f_{\mathbf{k}\sigma} + \tilde{V}_{\mathbf{k}} \left(c_{\mathbf{k}\sigma}^\dagger f_{\mathbf{k}\sigma} + h.c. \right) + \lambda(r^2 - 1). \quad (2)$$

The MF Hamiltonian can be diagonalized using the unitary transformation,

$$\begin{aligned} f_{\mathbf{k}\sigma} &= u_{+,\mathbf{k}\sigma} \alpha_{+,\mathbf{k}\sigma} + u_{-,\mathbf{k}\sigma} \alpha_{-,\mathbf{k}\sigma} \\ c_{\mathbf{k}\sigma} &= u_{-,\mathbf{k}\sigma} \alpha_{+,\mathbf{k}\sigma} - u_{+,\mathbf{k}\sigma} \alpha_{-,\mathbf{k}\sigma} \end{aligned} \quad (3)$$

and as a result one can find the MF quasiparticle Hamiltonian as

$$\mathcal{H}^{\text{MF}} = \sum_{\pm,\mathbf{k}\sigma} E_{\mathbf{k}\sigma}^{\pm} \alpha_{\pm,\mathbf{k}\sigma}^\dagger \alpha_{\pm,\mathbf{k}\sigma} + \lambda(r^2 - 1), \quad (4)$$

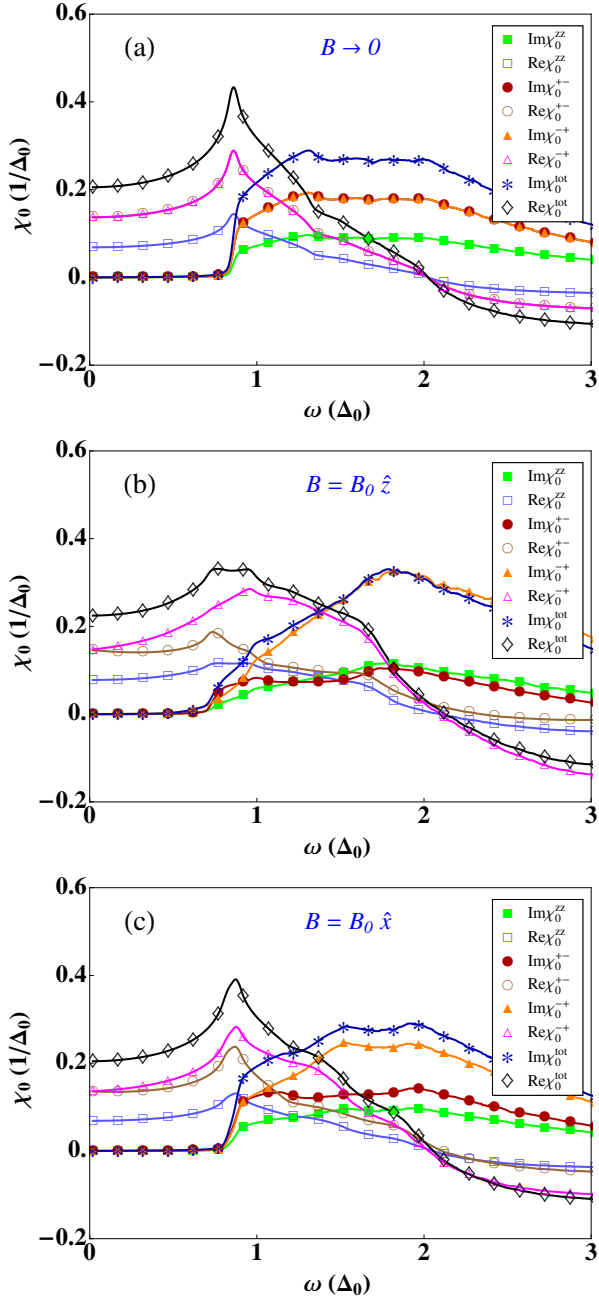


FIG. 2. (Color online) Individual compounds ($\chi_0^{ll'}$) and total (χ_0^{tot}) of the unperturbed pseudo spin susceptibility in absence (a) and at presence of the magnetic field along the \hat{z} direction (b), and for magnetic field along the \hat{x} direction (c). (B_0 is the same as Fig.1).

where the two pairs of quasiparticle bands (pairwise degenerate for zero field) are given by

$$E_{\mathbf{k}\sigma}^{\pm} = \frac{1}{2} \left[\varepsilon_{\mathbf{k}\sigma}^c + \tilde{\varepsilon}_{\mathbf{k}\sigma}^f \pm \sqrt{(\varepsilon_{\mathbf{k}\sigma}^c - \tilde{\varepsilon}_{\mathbf{k}\sigma}^f)^2 + 4\tilde{V}_{\mathbf{k}}^2} \right], \quad (5)$$

and the quasiparticle mixing amplitudes are obtained

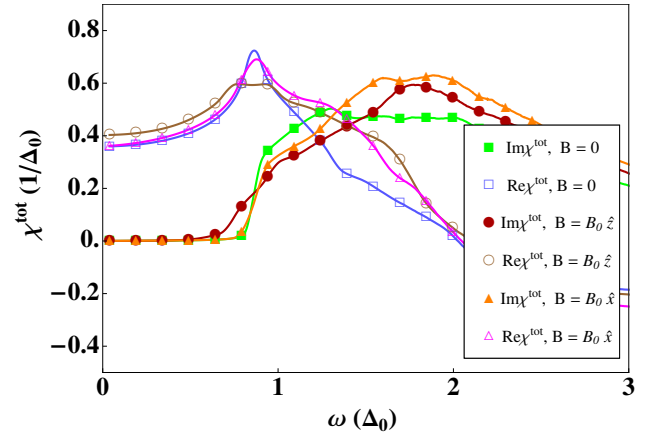


FIG. 3. (Color online) The total unperturbed physical susceptibility (including matrix elements m_{\parallel}, m_{\perp} ; $\chi^{tot}(\mathbf{Q}, \omega) = \chi^{zz} + \frac{1}{2}[\chi^{+-} + \chi^{-+}]$) for zero field and finite field along \hat{z} , and \hat{x} directions. (B_0 is the same as Fig.1).

from

$$u_{\pm, \mathbf{k}\sigma}^2 = \frac{1}{2} \left(1 \pm \frac{\varepsilon_{\mathbf{k}\sigma}^c - \tilde{\varepsilon}_{\mathbf{k}\sigma}^f}{\sqrt{(\varepsilon_{\mathbf{k}\sigma}^c - \tilde{\varepsilon}_{\mathbf{k}\sigma}^f)^2 + 4\tilde{V}_{\mathbf{k}}^2}} \right). \quad (6)$$

Using the parameters defined in Ref. 29 for the above quasiparticle band structure we plot the corresponding FS in Fig.1(a) in the absence of a magnetic field. Since the Fermi level is located in the lower band, $E_{\mathbf{k}\sigma}^-$, we can neglect the upper band, $E_{\mathbf{k}\sigma}^+$ for discussing the low energy spin excitations.

The superconducting pairs are then formed from the heavy quasiparticles of the lower band leading to a pairing potential in the Hamiltonian according to

$$\mathcal{H}^{SC} = \sum_{\mathbf{k}} \Delta_{\mathbf{k}} \left(\alpha_{-, \mathbf{k}\uparrow}^{\dagger} \alpha_{-, -\mathbf{k}\downarrow}^{\dagger} + h.c. \right), \quad (7)$$

where $\Delta_{\mathbf{k}}$ is the superconducting d-wave gap function for CeMIn₅ given by

$$\Delta_{\mathbf{k}} = \frac{\Delta_0}{2} (\cos k_x - \cos k_y). \quad (8)$$

By defining the new Nambu spinors as $\hat{\psi}_{\mathbf{k}}^{\dagger} = (\hat{\phi}_{1\mathbf{k}}^{\dagger}, \hat{\phi}_{2\mathbf{k}}^{\dagger})$, the effective Hamiltonian can be written as

$$\mathcal{H}^{eff} = \frac{1}{2} \sum_{\mathbf{k}} \hat{\psi}_{\mathbf{k}}^{\dagger} \hat{\beta}_{\mathbf{k}} \hat{\psi}_{\mathbf{k}}, \quad (9)$$

here $\hat{\phi}_{1\mathbf{k}}^{\dagger} = (\alpha_{-, \mathbf{k}\uparrow}^{\dagger}, \alpha_{-, \mathbf{k}\downarrow}^{\dagger})$, and $\hat{\phi}_{2\mathbf{k}}^{\dagger} = (\alpha_{-, -\mathbf{k}\uparrow}, \alpha_{-, -\mathbf{k}\downarrow})$ and

$$\hat{\beta}_{\mathbf{k}} = \begin{bmatrix} E_{\mathbf{k}\uparrow}^- & 0 & 0 & \Delta_{\mathbf{k}} \\ 0 & E_{\mathbf{k}\downarrow}^- & -\Delta_{\mathbf{k}} & 0 \\ 0 & -\Delta_{\mathbf{k}} & -E_{-\mathbf{k}\uparrow}^- & 0 \\ \Delta_{\mathbf{k}} & 0 & 0 & -E_{-\mathbf{k}\downarrow}^- \end{bmatrix}. \quad (10)$$

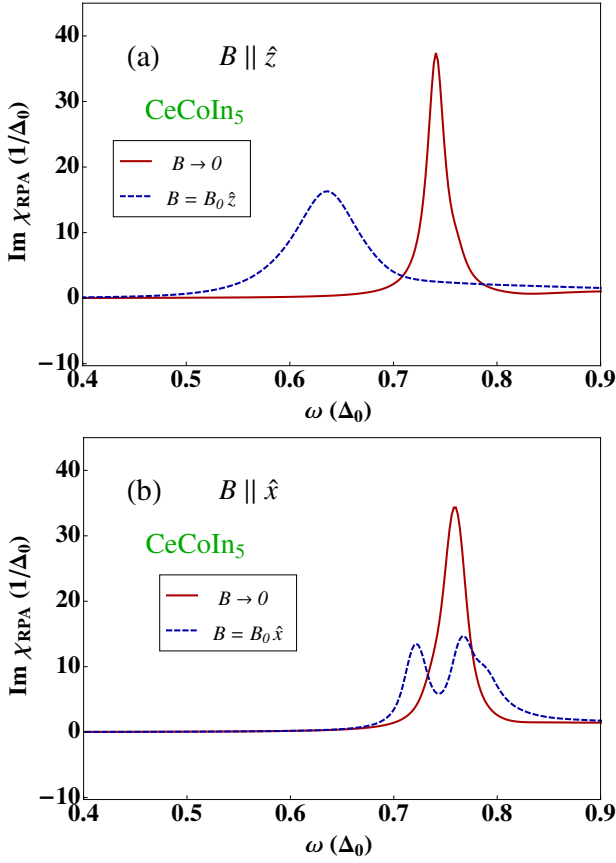


FIG. 4. (Color online) RPA susceptibility in absence and presence of the magnetic field: along the \hat{z} direction (a), and along the \hat{x} direction (b). Parameters corresponding to the behaviour as observed in CeCoIn₅ with $g_{\perp}^{\parallel}/g_{\parallel}^{\parallel} = 2.3$ and $J_{\mathbf{Q}}^{\perp} = 2.6\Delta_0$; $J_{\mathbf{Q}}^{\parallel} = 13.5\Delta_0$. (B_0 is the same as Fig.1).

The propagator matrix of the conduction electrons in terms of the Nambu spinor in the Matsubara representation is obtained as $\hat{G}(\mathbf{k}, \tau) = -\langle T \hat{\psi}_{\mathbf{k}}(\tau) \hat{\psi}_{\mathbf{k}}^{\dagger}(0) \rangle$. Using a standard equation of motion method one can find that

$$\hat{G}(\mathbf{k}, \omega_n) = \left(i\omega_n - \hat{\beta}_{\mathbf{k}} \right)^{-1}. \quad (11)$$

Explicitly written,

$$\hat{G}(\mathbf{k}, \tau) = \begin{bmatrix} \hat{G}_0^{11}(\mathbf{k}, \tau) & \hat{G}_0^{12}(\mathbf{k}, \tau) \\ \hat{G}_0^{21}(\mathbf{k}, \tau) & \hat{G}_0^{22}(\mathbf{k}, \tau) \end{bmatrix} \quad (12)$$

where $\hat{G}_0^{\zeta\zeta'}(\mathbf{k}, \tau) = -\langle T \hat{\phi}_{\zeta\mathbf{k}}(\tau) \hat{\phi}_{\zeta'\mathbf{k}}^{\dagger}(0) \rangle$ and $\zeta, \zeta' = 1, 2$ denote the spinor components for $\pm\mathbf{k}$ below Eq. (9).

A. Magnetic susceptibility

The noninteracting or bare dynamical f-electron susceptibility is defined by

$$\chi_{\mathbf{q}}^{ll'}(\tau) = -\theta(\tau) \langle T j_{\mathbf{q}}^l(\tau) j_{-\mathbf{q}}^{l'}(0) \rangle, \quad (13)$$

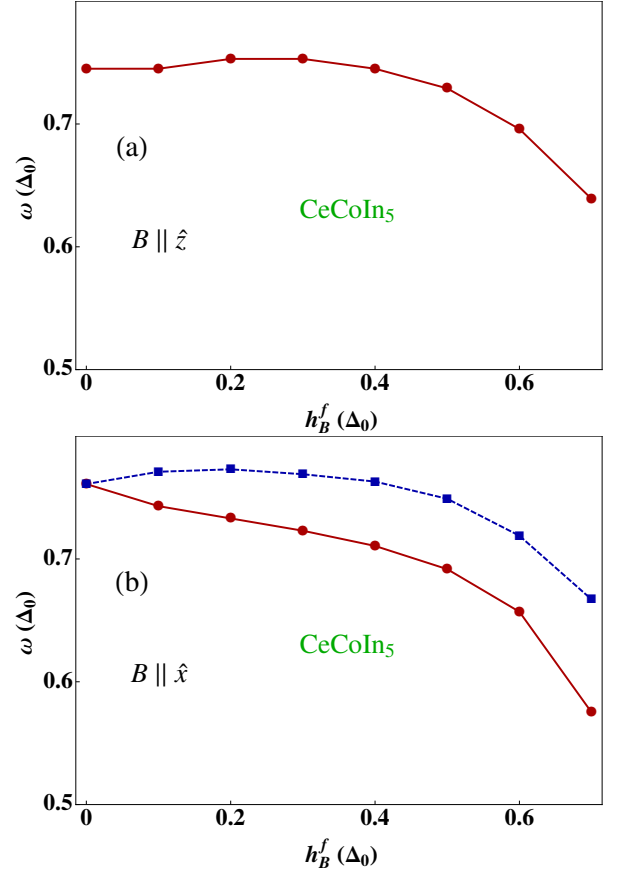


FIG. 5. (Color online) RPA susceptibility peak positions corresponding to spin resonance energies as function of field strength: along the \hat{z} direction (a), and along the \hat{x} direction (b). Anisotropic g- factors with $g_{\perp}^{\parallel}/g_{\parallel}^{\parallel} = 2.3$ and quasi-particle interaction parameters $J_{\mathbf{Q}}^{\perp} = 2.6\Delta_0$; $J_{\mathbf{Q}}^{\parallel} = 13.5\Delta_0$ leading to similar behaviour as in CeCoIn₅ for both field directions. Here the maximum $h_B^f = 0.7\Delta_0$ corresponds to a field $B = 39.7/(g_{\perp}^{\parallel}\tilde{\chi})$ in Tesla for direction $l = \perp, \parallel$.

where

$$j_{\mathbf{q}}^l = \sum_{\mathbf{k}\sigma\sigma'} f_{\mathbf{k}+\mathbf{q}\sigma}^{\dagger} \hat{M}_{\sigma\sigma'}^l f_{\mathbf{k}\sigma'}. \quad (14)$$

The hybridizing 4f states are in a $|\Gamma_7^{(1)}\rangle$ Kramers doublet state and therefore their physical moment operator (in units of μ_B) can be presented by a pseudo spin matrix σ according to ($l = +, -, z$)

$$\hat{M}_l = m_l \sigma_l \quad (15)$$

Here m_l are matrix elements and their anisotropy ($m_{\pm} = m_{\parallel}; m_z = m_{\perp}$) may be directly obtained from that of the experimental spin susceptibility of quasiparticles³² according to $m_{\perp}/m_{\parallel} = g_{\perp}^f/g_{\parallel}^f = (\chi_{\perp}^s/\chi_{\parallel}^s)^{\frac{1}{2}} = 2.3$. Their absolute value is not significant as it only sets the overall scale. Then, the bare physical moment susceptibility can be expressed as

$$\chi^{ll'}(\mathbf{q}, \omega) = m_l m_{l'} \chi_0^{ll'}(\mathbf{q}, \omega), \quad (16)$$

where $\chi_0^{ll'}(\mathbf{q}, \omega)$ is the pseudo spin susceptibility defined by

$$\chi_0^{ll'}(\mathbf{q}, \omega) = \sum_{\mathbf{k}, \{\sigma\}} \sigma_{\sigma\sigma'}^l \sigma_{\sigma_1\sigma_1'}^{l'} u_{-, \mathbf{k}+\mathbf{q}\sigma} u_{-, \mathbf{k}+\mathbf{q}\sigma_1'} u_{-, \mathbf{k}\sigma_1} u_{-, \mathbf{k}\sigma'} \int d\omega' \hat{G}_{0\sigma\sigma_1}^{11}(\mathbf{k}+\mathbf{q}, \nu+\omega') \hat{G}_{0\sigma_1\sigma_1'}^{11}(\mathbf{k}, \omega') |_{i\nu \rightarrow \omega+i0^+}. \quad (17)$$

With the definition of the new basis as $\hat{\varphi}_{\mathbf{k}}^\dagger = (b_{+,1\mathbf{k}}, b_{+,2\mathbf{k}}, b_{-,2\mathbf{k}}, b_{-,1\mathbf{k}})$ and applying the Bogoliubov transformation given by

$$\begin{aligned} \alpha_{-, \mathbf{k}\uparrow}^\dagger &= v_{+,1\mathbf{k}} b_{+,1\mathbf{k}} + v_{-,1\mathbf{k}} b_{-,1\mathbf{k}} \\ \alpha_{-, -\mathbf{k}\downarrow} &= -v_{-,1\mathbf{k}} b_{+,1\mathbf{k}} + v_{+,1\mathbf{k}} b_{-,1\mathbf{k}} \\ \alpha_{-, \mathbf{k}\downarrow}^\dagger &= v_{+,2\mathbf{k}} b_{+,2\mathbf{k}} - v_{-,2\mathbf{k}} b_{-,2\mathbf{k}} \\ \alpha_{-, -\mathbf{k}\uparrow} &= v_{-,2\mathbf{k}} b_{+,2\mathbf{k}} + v_{+,2\mathbf{k}} b_{-,2\mathbf{k}} \end{aligned} \quad (18)$$

the effective Hamiltonian in Eq. (9) is diagonalized by $\hat{\beta}_{\mathbf{k}}^d = P_{\mathbf{k}} \hat{\beta}_{\mathbf{k}} P_{\mathbf{k}}^{-1}$, where $P_{\mathbf{k}}$ is a 4×4 matrix, composed of the eigenvectors of $\hat{\beta}_{\mathbf{k}}$. Here $\hat{\beta}_{\mathbf{k}}^d$ is the diagonal matrix constructed from the corresponding eigenvalues,

$$\bar{E}_{1\mathbf{k}}^\pm = \bar{E}_{2,-\mathbf{k}}^\pm = \frac{1}{2} \left[E_{\mathbf{k}\uparrow}^- - E_{-\mathbf{k}\downarrow}^- \pm \sqrt{(E_{\mathbf{k}\uparrow}^- + E_{-\mathbf{k}\downarrow}^-)^2 + 4\Delta_{\mathbf{k}}^2} \right], \quad (19)$$

and $P_{\mathbf{k}}^{-1}$ is the matrix inverse of $P_{\mathbf{k}}$. Furthermore,

$$v_{\pm, 1\mathbf{k}}^2 = v_{\pm, 2, -\mathbf{k}}^2 = \frac{1}{2} \left(1 \pm \frac{E_{\mathbf{k}\uparrow}^- + E_{-\mathbf{k}\downarrow}^-}{\sqrt{(E_{\mathbf{k}\uparrow}^- + E_{-\mathbf{k}\downarrow}^-)^2 + 4\Delta_{\mathbf{k}}^2}} \right). \quad (20)$$

Then $\hat{G}^d(\mathbf{k}, \omega_n) = (i\omega_n - \hat{\beta}_{\mathbf{k}}^d)^{-1}$ is diagonal and we can write

$$\hat{G}_{0\sigma\sigma_1}^{11}(\mathbf{k}, \omega_n) = \sum_{s'=1}^4 \gamma_{\sigma\sigma_1 s'}^{\mathbf{k}} \hat{G}_{s'}^d(\mathbf{k}, \omega_n), \quad (21)$$

where $\gamma_{\sigma\sigma_1 s'}^{\mathbf{k}} = P_{\mathbf{k} s'}^{-1} P_{\mathbf{k} s' \sigma_1}$. Thus, the pseudo-spin susceptibility can now be expressed as

$$\chi_0^{ll'}(\mathbf{q}, \omega) = \sum_{\mathbf{k}, \{\sigma\}} \sum_{\{s\}} \sigma_{\sigma\sigma'}^l \sigma_{\sigma_1\sigma_1'}^{l'} \gamma_{\sigma\sigma_1 s_2}^{\mathbf{k}+\mathbf{q}} \gamma_{\sigma_1\sigma' s_2}^{\mathbf{k}} u_{-, \mathbf{k}+\mathbf{q}\sigma} u_{-, \mathbf{k}+\mathbf{q}\sigma_1'} u_{-, \mathbf{k}\sigma_1} u_{-, \mathbf{k}\sigma'} \frac{f(\hat{\beta}_{\mathbf{k}+\mathbf{q}, s_2}^d) - f(\hat{\beta}_{\mathbf{k}, s_2}^d)}{\omega - (\hat{\beta}_{\mathbf{k}+\mathbf{q}, s_2}^d - \hat{\beta}_{\mathbf{k}, s_2}^d)}, \quad (22)$$

where $f(\epsilon)$ is the Fermi function. The combination of prefactors in the sum of Eq. (22) are the combined coherence factors arising from the hybridisation and the superconducting state. Finally the cartesian dynamic magnetic susceptibility tensor in random phase approximation (RPA) has the form

$$\hat{\chi}_{RPA}(\mathbf{q}, \omega) = [1 - \hat{J}(\mathbf{q}) \hat{\chi}(\mathbf{q}, \omega)]^{-1} \hat{\chi}(\mathbf{q}, \omega), \quad (23)$$

where $\hat{J}(\mathbf{q})$ is the effective quasiparticle interaction matrix with non-zero elements: $J_{\mathbf{q}}^{zz} = J_{\mathbf{q}}^{\perp}$, $J_{\mathbf{q}}^{+-} = J_{\mathbf{q}}^{-+} = J_{\mathbf{q}}^{\parallel}$. Similar to the g-factors they may be anisotropic. Furthermore their momentum dependence can be modeled by a Lorentzian function which is peaked at the wave vector \mathbf{Q} associated with the indirect hybridization gap³⁵. Finally the total dynamic magnetic susceptibility is obtained as the trace of the tensor according to

$$\chi_{RPA}(\mathbf{q}, \omega) = \chi_{RPA}^{zz}(\mathbf{q}, \omega) + \frac{1}{2} [\chi_{RPA}^{+-}(\mathbf{q}, \omega) + \chi_{RPA}^{-+}(\mathbf{q}, \omega)]. \quad (24)$$

For momentum transfer \mathbf{q} along $\mathbf{Q} = (\frac{1}{2}, \frac{1}{2}, \frac{1}{2})$ direction this is directly proportional to the dynamical structure factor $S(\mathbf{q}, \omega)$ observed in INS experiments.

III. NUMERICAL RESULTS

In this section, we evaluate numerically the dynamic magnetic susceptibility for our model of 115 systems. We consider two different cases, namely magnetic field along \hat{z} -direction (out-of-plane: c-axis) and along \hat{x} -direction (in-plane: a-axis). For clarity we give first the relevant physical parameters of CeCoIn₅ to simplify comparison with experimental results. For the main (lower) tunneling gap (Fig. 1) we have $2\Delta_1 = 0.56\Delta_0 = 0.92\text{meV}^9$ or $\Delta_0 = 1.64\text{meV}$ for the gap amplitude in Eq. (8). The spin resonance energy for zero field is $\omega_r = 0.6\text{meV}^{10}$ or $\omega_r/2\Delta_1 \simeq 0.65$.

First, using Eq.(22), we calculate the individual components $\chi_0^{ll'}(\mathbf{Q}, \omega)$ of the pseudo-spin susceptibility tensor and its trace $\chi_0^{tot}(\mathbf{Q}, \omega) = \chi_0^{zz}(\mathbf{Q}, \omega) + \frac{1}{2}[\chi_0^{+-}(\mathbf{Q}, \omega) + \chi_0^{-+}(\mathbf{Q}, \omega)]$. For $B \rightarrow 0$ Fig.2.a shows that $\frac{1}{2}\chi_0^{+-}$, $\frac{1}{2}\chi_0^{-+}$ and χ_0^{zz} become identical, independent of the field direction due to isotropy in pseudo-spin space. Therefore χ_0^{tot} for $B \rightarrow 0$ in Fig.2.a is simply three times each of these components. This means that the anisotropy enters only through the matrix elements in the physical moment susceptibility of Eq. (16) discussed below. The pseudo-spin susceptibility in presence of a magnetic field along the \hat{z} -direction is shown in Fig.2.b and for \hat{x} -direction in Fig.2.c. We note here that for calculating the pseudo spin susceptibility with magnetic field along the \hat{x} -direction, we have applied a $\pi/2$ rotation along the \hat{y} -direction ($\hat{x} \rightarrow -\hat{z}$ and $\hat{z} \rightarrow \hat{x}$) and similar in \mathbf{k} -space. For finite field and both directions the individual components for each field direction start to differ because of the polarization of quasiparticle bands in the field. This leads to a change of the nesting conditions of the FS in presence of a magnetic field, shown in Fig.(1.b), which is different for each susceptibility component. Most importantly the energy dependence of χ_0^{+-} and χ_0^{-+} shows a splitting in opposite manner.

We also calculate the total bare physical susceptibility, $\chi^{tot}(\mathbf{Q}, \omega)$ resulting from Eq.(16) in Fig.3. The anisotropy enters only through the matrix elements m_{\parallel}, m_{\perp} in the physical moment susceptibility of

Eq. (16). It is shown at zero magnetic field ($B \rightarrow 0$), and also for magnetic field along \hat{z} - and \hat{x} -directions (in original axis notation), respectively. We note that for $B \rightarrow 0$ the $\frac{1}{2}\chi^{+-}$ and $\frac{1}{2}\chi^{-+}$ components are still equivalent as in Fig.2.a but differ from χ^{zz} due to the different magnetic moment for in plane and out-of-plane direction (see Eq.15).

Finally, from Eq.(24) the interacting RPA susceptibility and the spectrum of excitations given by its imaginary part can be calculated. In general form, we obtain

$$\chi_{RPA}(\mathbf{q}, \omega) = \frac{m_z^2 \chi_0^{zz}}{1 - \lambda_z \chi_0^{zz}} + \frac{(m_x^2 + m_y^2)(\chi_0^{+-} + \chi_0^{-+}) - (\lambda_x m_y^2 + \lambda_y m_x^2) \chi_0^{+-} \chi_0^{-+}}{4 - (\lambda_x + \lambda_y)(\chi_0^{+-} + \chi_0^{-+}) + \lambda_x \lambda_y \chi_0^{+-} \chi_0^{-+}}. \quad (25)$$

where the interaction parameters are defined as $\lambda_l = m_l^2 J_{\mathbf{q}}^l$ (here $l = x = y = \parallel, z = \perp$ for the original axes, and $l = z = y = \parallel, x = \perp$ for the rotated axes). If the resonance condition should be satisfied for both transverse parts in Eq.(24) then one must have $m_{\parallel}^2 J_{\mathbf{q}}^{\perp} \approx m_{\perp}^2 J_{\mathbf{q}}^{\parallel}$. Since the CEF states and hence the anisotropy may change as an effect of substitutions in the pure 115 compounds the resonance signatures may also change accordingly. As a result of the sign change of the superconducting gap function ($\Delta_{\mathbf{k}+\mathbf{Q}} = -\Delta_{\mathbf{k}}$) at the antiferromagnetic momentum \mathbf{Q} the spectral function $\text{Im}\chi_0(\mathbf{Q}, \omega)$ remains zero for the low frequencies and then shows a discontinuous jump at the onset frequency of the particle-hole (p-h) continuum, i.e., close to $\omega_c = \min(\Delta_{\mathbf{k}+\mathbf{Q}} + \Delta_{\mathbf{k}})$. This is around $\Delta_0 \simeq 2\Delta_1$, where $2\Delta_1$ is the gap in the superconducting DOS in (Fig.1.b) which is observed in the tunneling spectrum of CeCoIn₅⁹. The resonance may appear for energies $\omega < \omega_c$, under the condition that (i) $J_{\mathbf{q}}^{ll'} \text{Re}\chi_{0\mathbf{q}}^{ll'}(\omega) = 1$ and (ii) $\text{Im}\chi_{0\mathbf{q}}^{ll'}(\omega) \simeq 0$ ($ll' = +- , -+ , zz$).

We begin our discussion of numerical results by considering the strongly anisotropic case with $J_{\mathbf{Q}}^{\perp} \ll J_{\mathbf{Q}}^{\parallel}$. Only in this case, the resonance condition is satisfied for both $\chi_{0\mathbf{Q}}^{+-}$ and $\chi_{0\mathbf{Q}}^{-+}$ components and not for $\chi_{0\mathbf{Q}}^{zz}$, i.e., a resonance doublet is possible as observed in experiment. At zero magnetic field a single sharp peak for the degenerate resonance is observed which is shown in Fig.4. By applying the magnetic field the bare χ_0^{+-}, χ_0^{-+} susceptibilities start to split into an upper and lower branch (Figs. 2.b,c), and as a result the two resonance peaks of the doublet are revealed in the RPA frequency spectrum. Because of the anisotropic interaction, these peaks are completely distinguishable for in-plane magnetic field showing a linear Zeeman splitting for small fields. On the other hand they merge together for the out-of-plane field and a single broadened peak appears whose width increases with field. Using the procedure described above for various fields we obtain the peak positions of the RPA

spectrum versus magnetic field strength in Fig.5. For field oriented along the \hat{z} -direction (Fig.5.a) we always have a single peak with larger broadening, and by increasing the magnetic field the peak moves to lower energies. But for the magnetic field applied in \hat{x} -direction (Fig.5.b) the RPA result shows always two peaks with narrower line widths. When the field is increased these peaks show first a linear Zeeman splitting and one of them moves to larger and the other one to lower energies. Finally at large field nonlinear behaviour sets in and both start to move to lower energies. These results are in complete qualitative agreement with the experimental observation for CeCoIn₅²¹ at lower fields which have so far been used only. It is clear that the linear splitting observed must be modified when larger fields closer to the upper critical fields are applied. The absolute field scale at the maximum $h_B^f = 0.7\Delta_0$ is $B = 39.7/(g_f^l \tilde{\chi})$ in Tesla for direction $l = \parallel, \perp$. From a comparison with the experimental linear splitting region up to 6T $\ll H_{c2}^{\parallel}$ and the one in Fig.5a with $h_B^f \approx 0.35$ one gets the parameter $g_f^{\parallel} \tilde{\chi} = 3.3$. We note that the reference scale Δ_0 is only constant for fields small to the upper critical field ($H_{c2}^{\parallel} = 11.9$ T, $H_{c2}^{\perp} = 4.95$ T). For larger fields one has to scale with $\Delta_0(B)$ which vanishes at the upper critical fields $H_{c2}^{\parallel, \perp}$ where the resonance energies $\omega_r(B)$ also have to vanish for both field directions. When the curves in Fig. 5a,b are multiplied by the scaling function $\Delta_0(B)$ the field dependence $\omega_r(B)$ is obtained in absolute (meV) units.

Finally we mention here that our results within the phenomenological RPA theory depend on the model parameters, i.e. anisotropic matrix elements and quasiparticle interaction energies. Changing these parameters leads to other interesting regimes, where the anisotropies of magnetic moment and quasiparticle interaction along the tetragonal axes play the decisive role. The RPA treatment shows that even in absence of the magnetic field an additional peak from the $\chi_{0\mathbf{q}}^{zz}$ component may appear for suitable parameters and therefore in principle two peaks may exist in the RPA spectrum even at zero field. In the presence of the magnetic field like previous cases the degenerate (doublet) peak of the $\chi_{0\mathbf{q}}^{+-}$ and $\chi_{0\mathbf{q}}^{-+}$ components splits and finally leading to three different peaks at finite field. We should stress here that by moving to lower interaction energy the resonance occurs just for $\chi_{0\mathbf{q}}^{-+}$ and the splitting of the resonance vanishes. This could give an insight into the challenging alternative experiments where the splitting behavior for in-plane field has not been seen²².

IV. CONCLUSION

We have given an explanation of the observed field splitting of feedback spin resonance excitations recently observed for the first time in the unconventional superconductor CeCoIn₅. Our calculations are based on a RPA

model with tetragonal anisotropy for collective spin excitations that may also be relevant for other members of the 115 family. Using the appropriate hybridized bands and associated Fermi surface as well as the proper $d_{x^2-y^2}$ superconducting gap symmetry the spin resonance appears at $\omega/2\Delta_1 = 0.73$, close to the experimental value. Here $2\Delta_1$ is the main tunneling gap indicated in the DOS of Fig.1.b and found in Ref. 9.

In the isotropic case the resonance is a spin triplet excitation that should split into three modes in a field as predicted in the case of a cuprate model²⁰. However, because of the presence of strong CEF and hybridization induced anisotropies of g-factors and interactions of 4f-type quasiparticles in 115 compounds the resonance condition may in this case not be fulfilled for all three triplet components. For sufficiently strong anisotropy the zero field resonance is only twofold degenerate transverse doublet state because the longitudinal component does not satisfy the resonance condition. For field in the tetrag-

onal plane the doublet splits with a linear Zeeman effect for low fields, one branch moving to higher the other two lower energies. However, for larger fields a crossover to nonlinear field dependence with both split resonance energies decreasing sets in. For field perpendicular to the tetragonal plane no splitting but only a broadening of the doublet resonance excitation appears. These salient features of our model calculation correspond closely to the experimental observations in CeCoIn₅ performed for small fields²¹. It would be very interesting to investigate the predicted nonlinear field dependence for larger fields.

Finally we note that other scenarios are possible depending on the anisotropies and strengths of quasiparticle interactions where for example the in-plane splitting of the resonance disappears and a single peak with anomalous broadening as for the out-of-plane field is observed. In fact this behaviour was proposed in an alternative experiment²² and further experimental as well as theoretical investigations are necessary to clarify this issue.

-
- * akbari@cpfs.mpg.de
- ¹ J. Thompson, R. Movshovich, Z. Fisk, F. Bouquet, N. Curro, R. Fisher, P. Hammel, H. Hegger, M. Hundley, M. Jaime, P. Pagliuso, C. Petrovic, N. Phillips, and J. Sarrao, *Journal of Magnetism and Magnetic Materials*, **226–230**, 5 (2001).
 - ² V. S. Zapf, E. J. Freeman, E. D. Bauer, J. Petricka, C. Sirvent, N. A. Frederick, R. P. Dickey, and M. B. Maple, *Phys. Rev. B*, **65**, 014506 (2001).
 - ³ J. L. Sarrao and J. D. Thompson, *Journal of the Physical Society of Japan*, **76**, 051013 (2007).
 - ⁴ J. D. Thompson and Z. Fisk, *Journal of the Physical Society of Japan*, **81**, 011002 (2012).
 - ⁵ A. Bianchi, R. Movshovich, C. Capan, P. G. Pagliuso, and J. L. Sarrao, *Phys. Rev. Lett.*, **91**, 187004 (2003).
 - ⁶ C. Petrovic, P. G. Pagliuso, M. F. Hundley, R. Movshovich, J. L. Sarrao, J. D. Thompson, Z. Fisk, and P. Monthoux, *Journal of Physics: Condensed Matter*, **13**, L337 (2001).
 - ⁷ K. Izawa, H. Yamaguchi, Y. Matsuda, H. Shishido, R. Settai, and Y. Onuki, *Phys. Rev. Lett.*, **87**, 057002 (2001).
 - ⁸ K. An, T. Sakakibara, R. Settai, Y. Onuki, M. Hiragi, M. Ichioka, and K. Machida, *Phys. Rev. Lett.*, **104**, 037002 (2010).
 - ⁹ P. M. C. Rourke, M. A. Tanatar, C. S. Turel, J. Berdeklis, C. Petrovic, and J. Y. T. Wei, *Phys. Rev. Lett.*, **94**, 107005 (2005).
 - ¹⁰ C. Stock, C. Broholm, J. Hudis, H. J. Kang, and C. Petrovic, *Phys. Rev. Lett.*, **100**, 087001 (2008).
 - ¹¹ I. Eremin, G. Zwirnagl, P. Thalmeier, and P. Fulde, *Phys. Rev. Lett.*, **101**, 187001 (2008).
 - ¹² N. Bulut and D. J. Scalapino, *Phys. Rev. B*, **53**, 5149 (1996).
 - ¹³ J. Rossat-Mignod, L. Regnault, C. Vettier, P. Bourges, P. Burllet, J. Bossy, J. Henry, and G. Lapertot, *Physica C: Superconductivity*, **185–189**, 86 (1991).
 - ¹⁴ N. K. Sato, N. Aso, K. Miyake, R. Shiina, P. Thalmeier, G. Varelogiannis, C. Geibel, F. Steglich, P. Fulde, and T. Komatsubara, *Nature*, **410**, 340 (2001).
 - ¹⁵ N. Metoki, Y. Haga, Y. Koike, N. Aso, and Y. Onuki, *Journal of the Physical Society of Japan*, **66**, 2560 (1997).
 - ¹⁶ J. Chang, I. Eremin, P. Thalmeier, and P. Fulde, *Phys. Rev. B*, **75**, 024503 (2007).
 - ¹⁷ O. Stockert, J. Arndt, A. Schneidewind, H. Schneider, H. Jeevan, C. Geibel, F. Steglich, and M. Loewenhaupt, *Physica B: Condensed Matter*, **403**, 973 (2008).
 - ¹⁸ O. Stockert, J. Arndt, E. Faulhaber, C. Geibel, H. S. Jeevan, S. Kirchner, M. Loewenhaupt, K. Schmalzl, W. Schmidt, Q. Si, and F. Steglich, *Nat Phys*, **7**, 119 (2011).
 - ¹⁹ A. D. Christianson, E. A. Goremychkin, R. Osborn, S. Rosenkranz, M. D. Lumsden, C. D. Malliakas, I. S. Todorov, H. Claus, D. Y. Chung, M. G. Kanatzidis, R. I. Bewley, and T. Guidi, *Nature*, **456**, 930 (2008).
 - ²⁰ J.-P. Ismer, I. Eremin, E. Rossi, and D. K. Morr, *Phys. Rev. Lett.*, **99**, 047005 (2007).
 - ²¹ C. Stock, C. Broholm, Y. Zhao, F. Demmel, H. J. Kang, K. C. Rule, and C. Petrovic, arXiv:1203.2189 (2012).
 - ²² J. Panarin, S. Raymond, G. Lapertot, J. Flouquet, and J.-M. Mignot, *Phys. Rev. B*, **84**, 052505 (2011).
 - ²³ J. Panarin, S. Raymond, G. Lapertot, and J. Flouquet, *Journal of the Physical Society of Japan*, **78**, 113706 (2009).
 - ²⁴ Y. Yanase and M. Sigrist, *Journal of the Physical Society of Japan*, **78** (2009).
 - ²⁵ A. Aperis, G. Varelogiannis, and P. B. Littlewood, *Physical Review Letters*, **104**, 216403 (2010).
 - ²⁶ M. Kenzelmann, S. Gerber, N. Egetenmeyer, J. L. Gavilano, T. Strässle, A. D. Bianchi, E. Ressouche, R. Movshovich, E. D. Bauer, J. L. Sarrao, and J. D. Thompson, *Phys. Rev. Lett.*, **104**, 127001 (2010).
 - ²⁷ K. Kumagai, H. Shishido, T. Shibauchi, and Y. Matsuda, arXiv:1103.1440.
 - ²⁸ V. P. Michal and V. P. Mineev, *Phys. Rev. B*, **84**, 052508 (2011).

- ²⁹ K. Tanaka, H. Ikeda, Y. Nisikawa, and K. Yamada, Journal of the Physical Society of Japan, **75**, 024713 (2006).
- ³⁰ T. Maehira, T. Hotta, K. Ueda, and A. Hasegawa, Journal of the Physical Society of Japan, **72**, 854 (2003).
- ³¹ A. D. Christianson, E. D. Bauer, J. M. Lawrence, P. S. Riseborough, N. O. Moreno, P. G. Pagliuso, J. L. Sarrao, J. D. Thompson, E. A. Goremychkin, F. R. Trouw, M. P. Hehlen, and R. J. McQueeney, Phys. Rev. B, **70**, 134505 (2004).
- ³² T. Tayama, A. Harita, T. Sakakibara, Y. Haga, H. Shishido, R. Settai, and Y. Onuki, Phys. Rev. B, **65**, 180504 (2002).
- ³³ A. Akbari, P. Thalmeier, and I. Eremin, Phys. Rev. B, **84**, 134505 (2011).
- ³⁴ A. Akbari and P. Thalmeier, Phys. Rev. Lett., **108**, 146403 (2012).
- ³⁵ A. Akbari, P. Thalmeier, and P. Fulde, Phys. Rev. Lett., **102**, 106402 (2009).